Effects of diffraction efficiency on the modulation transfer function of diffractive lenses

Dale A. Buralli and G. Michael Morris

Diffractive lenses differ from conventional optical elements in that they can produce more than one image because of the presence of more than one diffraction order. These spurious, defocused images serve to lower the contrast of the desired image. We show that a quantity that we define as the integrated efficiency serves as a useful figure of merit to describe diffractive lenses. The integrated efficiency is shown to be the limiting value for the optical transfer function; in most cases it serves as an overall scale factor for the transfer function. We discuss both monochromatic and polychromatic applications of the integrated efficiency and provide examples to demonstrate its utility.

1. Introduction

Recent advances in manufacturing techniques[1–3] have brought about many interesting developments in diffractive optical elements.[4] The ability to produce an arbitrary wave front with a diffractive element gives the optical designer a powerful tool to use in the design of modern optical systems. However, in addition to the normal considerations of focal length, aberration correction, and the like, with diffractive optics the designer must also be aware of the effects that diffraction efficiency has on the image-forming characteristics of the lens. The usual scalar-diffraction-theory treatment of diffractive lenses indicates that with the proper surface profile, surface-relief diffractive lenses (or kinoforms) should be capable of diffracting 100% of the incident energy into a single diffraction order.[5] However, results from rigorous electromagnetic grating theory indicate that diffraction efficiencies of less than 100% can be expected,[6] particularly when the grating period is of the same order as the wavelength of the light. Thus we expect the efficiency of a diffractive lens to vary across the area of the lens as the ratio of wavelength to grating period changes. In addition to these deviations of diffraction efficiency from the scalar-theory prediction, if the diffractive lens is used in spectrally broadband light, even the scalar theory predicts efficiencies of less than 100% when the wavelength is changed from the design wavelength. In the general case the efficiency of a diffractive lens is a function of both pupil position and wavelength.

The effect of nonunity diffraction efficiency is illustrated schematically in Fig. 1. The energy diffracted into the order of interest is focused to form the primary component of the point-spread function, while the other orders, generally largely out of focus, form a background of comparatively large spatial extent.

The purpose of this paper is to show, once the diffraction efficiency is known, how to quantify the effects of non-100% efficiency on the optical transfer function of systems that may contain diffractive lenses. We show that a quantity that we call the integrated efficiency serves as a useful figure of merit for evaluating diffractive lenses. This integrated efficiency describes the deterministic loss of energy into background diffraction orders, not the effects of random-surface scatter. Section 2 introduces the concept and definition of integrated efficiency. The relationship of integrated efficiency and the optical transfer function is explored in Section 3 and an illustrative example is presented in Section 4. In Section 5, we conclude with an extension to broadband systems by introducing the polychromatic integrated efficiency. In this paper we do not attempt to provide a rigorous prediction of diffraction efficiency for a diffractive lens. The diffraction efficiency will depend on the particular optical system parameters being considered: wavelength, lens material, angle(s) of incidence, polarization, and so on. Interested readers are referred to the literature on rigorous grating theories if they wish to investigate the

When this work was done the authors were with the Institute of Optics, University of Rochester, Rochester, New York 14627. D. A. Buralli is now with Sinclair Optics, Inc., 6780 Pittsford-Palmyra Road, Fairport, New York 14450.

Received March 25, 1991.
0003-6935/92/224389-08$05.00/0.

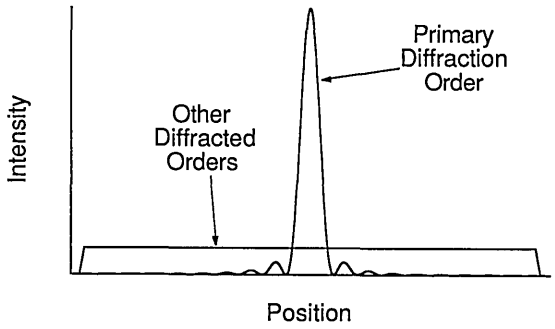

Fig. 1. Schematic illustration of the point-spread function for an optical system that contains diffractive elements. The point-spread function comprises two components: a focused component caused by the diffraction order of interest and a background component, not necessarily uniform, of large spatial extent caused by the other diffraction orders.

complicated interrelationships of the parameters governing grating efficiency.

2. Definition of Integrated Efficiency

Throughout this paper we will refer to a quantity that we call the integrated efficiency, η_{int}. In this section we define this quantity so that in the following sections we can see its relationship to meaningful imaging-performance measures. Our analysis is based on a linear systems approach, which has proved useful in assessing the effects of stray light in optical system performance.[7–9] Although the pupil function for a system that contains diffractive optics will generally be a complicated function because of the possible presence of many diffracted orders, for our purposes we shall consider the pupil function to consist of two components. One part of the pupil function is for the diffracted order of interest, i.e., the order that forms the desired image. We shall call this term the $m = 1$ term because usually it is the first diffracted order that is used, although in this context the $m = 1$ designation is strictly a label. The other component of the pupil function is caused by the other diffracted orders that propagate to the exit pupil and hence to the image. These other orders will be denoted by the term BG, because these orders serve to provide a background level of illumination in the image plane. Thus, if we denote the amplitude transmittance by t and the wave-front aberration (optical path difference) by W, we can write the pupil function P as a function of pupil coordinates u and v as

$$P(u, v) = t_{m=1}(u, v)\exp\left[i\frac{k}{n'}W_{m=1}(u, v)\right] + t_{\text{BG}}(u, v)\exp\left[i\frac{k}{n'}W_{\text{BG}}(u, v)\right], \quad (1)$$

where $k = 2\pi/\lambda$, λ is the vacuum wavelength of the light and n' is the image-space refractive index. The squared modulus of the $m = 1$ term is the local diffraction efficiency, η_{local}, i.e., the diffraction efficiency at the point (u, v) in the pupil:

$$\eta_{\text{local}}(u, v) = |t_{m=1}(u, v)|^2. \quad (2)$$

We define the integrated efficiency η_{int} as the pupil-averaged value of η_{local}, i.e.,

$$\eta_{\text{int}} = \frac{1}{A_{\text{pupil}}}\int_{-\infty}^{\infty}\int_{-\infty}^{\infty}\eta_{\text{local}}(u, v)\,du\,dv, \quad (3)$$

where A_{pupil} is the area of the exit pupil and $\eta_{\text{local}}(u, v) \equiv 0$ for points (u, v) outside the boundary of the pupil.

The point-spread function $I(x, y)$ corresponding to the pupil function $P(u, v)$ is the squared modulus of the Fourier transform of the pupil function, with spatial frequencies corresponding to scaled displacements in the image plane.[10] We can define two amplitude-impulse responses corresponding to the two components of $P(u, v)$, which we call $h_{m=1}(x, y)$ and $h_{\text{BG}}(x, y)$. These amplitude-impulse responses are given by (assuming $n' = 1$ for simplicity)[11]

$$h_{m=1}(x, y) = \frac{1}{\lambda R}\int_{-\infty}^{\infty}\int_{-\infty}^{\infty}t_{m=1}(u, v)\exp[ikW_{m=1}(u, v)] \times \exp\left[\frac{-i2\pi}{\lambda R}(xu + yv)\right]du\,dv, \quad (4a)$$

$$h_{\text{BG}}(x, y) = \frac{1}{\lambda R}\int_{-\infty}^{\infty}\int_{-\infty}^{\infty}t_{\text{BG}}(u, v)\exp[ikW_{\text{BG}}(u, v)] \times \exp\left[\frac{-i2\pi}{\lambda R}(xu + yv)\right]du\,dv, \quad (4b)$$

where R is the radius of the reference sphere, i.e., the distance from the exit pupil to the image plane. The point-spread function is then the squared modulus of the sum of the amplitude-impulse responses:

$$I(x, y) = |h_{m=1}(x, y)|^2 + |h_{\text{BG}}(x, y)|^2 + h_{m=1}{}^*(x, y)h_{\text{BG}}(x, y) + h_{m=1}(x, y)h_{\text{BG}}{}^*(x, y). \quad (5)$$

In Eq. (5) the asterisk denotes the complex conjugate. The cross terms in the expression for the intensity given in Eq. (5) will affect the intensity at an image point (x, y) in a small way. However, for the purposes of this paper, we are only interested in their effects on the calculation of the optical transfer function (OTF). Because the spatial extent of $h_{\text{BG}}(x, y)$ will generally be much larger than that of $h_{m=1}(x, y)$, we expect that the contribution of the background terms to the OTF will be significant only near the origin of the OTF. The value at the origin of the OTF is proportional to the integral of Eq. (5) over all x and y. The analysis in Appendix A shows that these integrals of the cross terms are zero. Note that even though the appendix considers the case of a one-dimensional function, a nonlinear limiter analysis[12] shows that the conclusions of the

appendix are valid for our case of interest—a rotationally symmetric diffractive lens. Thus, for the purposes of approximating the OTF for a diffractive lens, these small cross terms may be ignored.

From the analysis in the appendix we see that for most cases of interest, the small cross terms in Eq. (5) can be ignored and we can write the point-spread function as

$$I(x, y) \cong |h_{m=1}(x, y)|^2 + |h_{BG}(x, y)|^2. \quad (6)$$

The form of the point-spread function has been illustrated schematically in Fig. 1. It is convenient to normalize the components of the point-spread function by A_{pupil} so that the total amount of energy in the point-spread function is unity. We denote these normalized point-spread function components by the superscript 1 so that

$$\int_{-\infty}^{\infty}\int_{-\infty}^{\infty} |h_{m=1}{}^1(x, y)|^2 dx dy + \int_{-\infty}^{\infty}\int_{-\infty}^{\infty} |h_{BG}{}^1(x, y)|^2 dx dy = 1, \quad (7)$$

$$I^1(x, y) \cong |h_{m=1}{}^1(x, y)|^2 + |h_{BG}{}^1(x, y)|^2. \quad (8)$$

Because $h_{m=1}(x, y)$ and $t_{m=1}(u, v)\exp[ikW_{m=1}(u, v)]$ are a Fourier transform pair, it follows from Eqs. (2), (3), (4), and (7) that

$$\eta_{int} = \int_{-\infty}^{\infty}\int_{-\infty}^{\infty} |h_{m=1}{}^1(x, y)|^2 dx dy. \quad (9)$$

Equation (9) is just a statement that η_{int} is the fraction of energy in the focused component of the point-spread function.

3. η_{int} and the Optical Transfer Function

In this section we quantify the effects of nonunity diffraction efficiency on the OTF. The optical transfer function $OTF(f_x, f_y)$ as a function of spatial frequencies f_x and f_y is the Fourier transform of the point-spread function $I^1(x, y)$:

$$OTF(f_x, f_y) = \int_{-\infty}^{\infty}\int_{-\infty}^{\infty} I^1(x, y) \times \exp[-i2\pi(f_x x + f_y y)] dx dy. \quad (10)$$

We can separate the OTF into two components corresponding to the $m = 1$ and BG terms:

$$OTF(f_x, f_y) = OTF_{m=1}(f_x, f_y) + OTF_{BG}(f_x, f_y). \quad (11)$$

It is instructive to examine the low-frequency behavior of the transfer function. Obviously, at $f_x = f_y = 0$ the OTF must be equal to one. This assumption can be verified by setting $f_x = f_y = 0$ in Eq. (10) and using the expression for $I^1(x, y)$ given in relation (8):

$$OTF(0, 0) = \int_{-\infty}^{\infty}\int_{-\infty}^{\infty} |h_{m=1}{}^1(x, y)|^2 dx dy + \int_{-\infty}^{\infty}\int_{-\infty}^{\infty} |h_{BG}{}^1(x, y)|^2 dx dy = 1. \quad (12)$$

In terms of the two components of the OTF we have

$$OTF_{m=1}(0, 0) = \eta_{int}, \quad (13a)$$

$$OTF_{BG}(0, 0) = 1 - \eta_{int}. \quad (13b)$$

The Taylor expansion of $OTF_{m=1}(f_x, f_y)$ around $f_x = f_y = 0$ is

$$OTF_{m=1}(f_x, f_y) = OTF_{m=1}(0, 0) + \left[\frac{\partial OTF_{m=1}}{\partial f_x}\right]_{f_x = f_y = 0} f_x + \left[\frac{\partial OTF_{m=1}}{\partial f_y}\right]_{f_x = f_y = 0} f_y + \cdots. \quad (14)$$

Thus we see from Eqs. (13a) and (14) the important result that, for the diffracted order of interest, η_{int} is the limiting value of the transfer function for the $m = 1$ component as f_x and f_y tend to zero. At zero spatial frequency the OTF is equal to unity, but for small, nonzero frequencies the transfer function for the $m = 1$ order tends toward η_{int} rather than one.

In many cases we can take this analysis one step further. Let us assume that, in the image plane, the background orders have a much larger spatial extent than the order of interest. This is a reasonable assumption, because the order of interest is being used to form an image and the background orders form (generally) extremely out-of-focus images. These background orders create optical systems of different focal lengths that operate concurrently with the system utilizing the order of interest. If, in image space, the background has a much *larger* spatial extent of nonnegligible irradiance than the focused order, then in the transfer function space it follows that the background has a much *smaller* extent than the order of interest. This conclusion is drawn from the fact that the transfer function and point-spread function are a Fourier transform pair. Hence, to a good approximation, the background orders contribute to the transfer function only at very low (near zero) spatial frequencies, with a value of $1 - \eta_{int}$ from Eq. (13b). Strictly speaking, of course, we need to know the functional form of $h_{BG}(x, y)$ to calculate the transfer function accurately. However, for simplicity, the earlier analysis of this paper indicates that we can, for the purposes of approximating the OTF, treat the effect of the background terms on the OTF as a Kronecker delta. Denoting $t_{m=1}(u, v)\exp[ikW_{m=1}(u, v)]$ by $P_{m=1}(u, v)$, we can write an approximate expression for the transfer function as

$$OTF(f_x, f_y) \cong \frac{1}{A_{pupil}}\int_{-\infty}^{\infty}\int_{-\infty}^{\infty} P_{m=1}(u, v) \otimes P_{m=1}(u, v) du dv + (1 - \eta_{int})\delta_{f_x,0}\delta_{f_y,0}, \quad (15)$$

where $\otimes$ is the autocorrelation operator and $\delta_{\alpha,\beta}$ is the Kronecker delta. We restate that relation (15) is an

approximate expression for the OTF: it is valid when the background terms have a much larger spatial extent than the focused diffraction order. If the true functional forms of the background terms were known, a more accurate expression for the transfer function could be found by Fourier transformation. Using the definition of η_{int} given by Eq. (3), relation (15) can be rewritten as

$$\mathrm{OTF}(f_x, f_y) \cong \frac{\eta_{int}\int_{-\infty}^{\infty}\int_{-\infty}^{\infty} P_{m=1}(u, v) \otimes P_{m=1}(u, v)\,du\,dv}{\int_{-\infty}^{\infty}\int_{-\infty}^{\infty} |t_{m=1}(u, v)|^2\,du\,dv} + (1 - \eta_{int})\delta_{f_x,0}\delta_{f_y,0}. \quad (16)$$

From relation (16), we see that the transfer function consists of a component caused by the $m = 1$ pupil function, scaled by η_{int}, with a spike at zero spatial frequency.[13] A major effect of the background orders is to reduce the contrast, particularly at lower spatial frequencies. That the contrast should be reduced by the background orders is no surprise, because it can be thought of as stray light, albeit stray light produced by the optical system itself. The important result is that the effects on the image of this stray light can be quantified with a single parameter that is directly related to the diffractive optical-element performance—the integrated diffraction efficiency, η_{int}.

4. Example of Diffraction-Efficiency Effects on Imaging

It has been found, both experimentally and theoretically, that the diffraction efficiency of a diffractive lens is a function of radial position on the lens.[14] This deviation from the scalar prediction of 100% efficiency is generally caused by both fabrication errors and possible nonvalidity of the scalar theory. For example, for f-numbers less than ~ 10, even a perfectly constructed diffractive lens exhibits a variation of efficiency with radial position. This variation results from the facts that faster lenses have smaller zone widths, and that as the grating period becomes smaller (with respect to wavelength), the scalar-diffraction theory is no longer adequate to describe the efficiency. For example, a recent paper[15] showed that for diffractive lenses used in the 8- to 12-μm thermal-infrared spectral region, the diffraction efficiency is approximately a linear function of radial position. In this section, we provide an example of the performance of a diffractive lens with a particular choice of the variation of diffraction efficiency with radial position. We have chosen forms for the local diffraction efficiency that are mathematically convenient, qualitatively consistent with the known behavior of actual lenses, and that illustrate the conclusions drawn in Section 3. The reader interested in the performance of particular diffractive lenses will, of course, need to determine the pertinent efficiency functions.

For simplicity, let us consider a one-dimensional example in which the pupil function contains only the $m = 1$ order and a single background-order component. We further assume that the $m = 1$ order is aberration free. Thus any departure of the OTF from the diffraction limit will be solely caused by the effects of nonunity diffraction efficiency. The optical system is schematically shown in Fig. 2, wherein a single diffractive lens is used to image an infinitely distant object. In this case, the $m = 0$ and $m = 2$ orders (which will usually be the highest-efficiency background orders) are (geometrically) the same size as the pupil. Thus, we will approximate the background term as just the geometric projection of the exit pupil on the image plane. This is a good approximation for points deep within the region of Fresnel diffraction.[16] For computational simplicity, we choose the amplitude-transmission functions as

$$t_{m=1}(u) = \cos(au), \quad (17a)$$

$$t_{BG}(u) = |\sin(au)|. \quad (17b)$$

In Eqs. (17) a is a parameter that describes the pupil dependence of the local diffraction efficiency, which is

$$\eta_{local}(u) = \cos^2(au). \quad (18)$$

We would expect the larger values of a to correspond to faster-speed lenses, which have larger wavelength-to-grating period ratios and larger departures from the unity diffraction efficiency predicted by simple scalar theory. The integrated efficiency resulting from the local efficiency of Eq. (18) is easily found to be

$$\eta_{int} = \frac{1}{2}\left[1 + \frac{\sin(aD)}{aD}\right], \quad (19)$$

where D is the width of the one-dimensional pupil. For our example pupil width of $D = 20$ mm, the local efficiency as a function of pupil coordinate is shown in Fig. 3, for several values of the parameter a.

The amplitude-impulse response is given by the Fourier transform of the $m = 1$ pupil function, Eq.

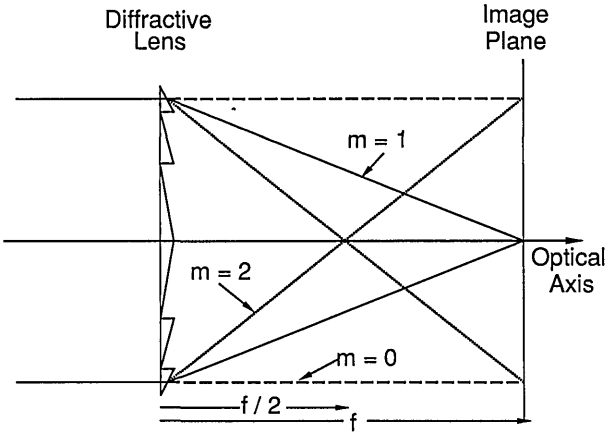

Fig. 2. Optical layout of single diffractive lens that images an infinitely distant object. The annotation m refers to the order of diffraction.

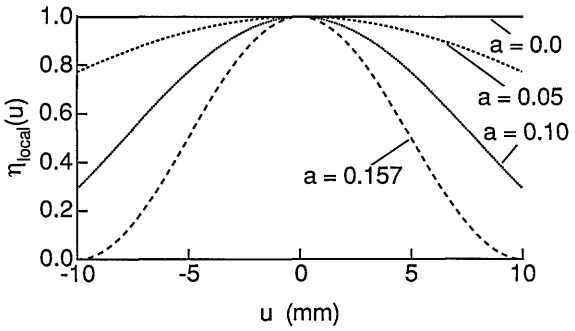

Fig. 3. Local diffraction efficiency as a function of pupil coordinate u for the imaging example discussed in the text. The pupil width is $D = 20$ mm, the exit pupil–image plane distance is $R = 100$ mm, the wavelength is $\lambda = 0.5$ μm, and the local diffraction efficiency is $\eta_{local}(u) = \cos^2(au)$.

(17a), and the geometric projection of the background pupil function, Eq. (17b). Performing this operation and taking the squared modulus yields, for the point-spread function,

$$I(x) = \frac{1}{D^2}\left\{\frac{\sin^2\left[\left(a - \frac{2\pi x}{\lambda R}\right)\frac{D}{2}\right]}{\left(a - \frac{2\pi x}{\lambda R}\right)^2} + \frac{\sin^2\left[\left(a + \frac{2\pi x}{\lambda R}\right)\frac{D}{2}\right]}{\left(a + \frac{2\pi x}{\lambda R}\right)^2}\right\}$$

$$+\frac{1}{D^2}\left\{\frac{\cos\left(\frac{2\pi Dx}{\lambda R}\right) - \cos(aD)}{\left(a - \frac{2\pi x}{\lambda R}\right)\left(a + \frac{2\pi x}{\lambda R}\right)} + \lambda R \sin^2(ax)\right\},$$

$$|x| \le (D/2), \tag{20a}$$

$$I(x) = \frac{1}{D^2}\left\{\frac{\sin^2\left[\left(a - \frac{2\pi x}{\lambda R}\right)\frac{D}{2}\right]}{\left(a - \frac{2\pi x}{\lambda R}\right)^2} + \frac{\sin^2\left[\left(a + \frac{2\pi x}{\lambda R}\right)\frac{D}{2}\right]}{\left(a + \frac{2\pi x}{\lambda R}\right)^2}\right.$$

$$\left. + \frac{\cos\left(\frac{2\pi Dx}{\lambda R}\right) - \cos(aD)}{\left(a - \frac{2\pi x}{\lambda R}\right)\left(a + \frac{2\pi x}{\lambda R}\right)}\right\}, \qquad |x| > (D/2). \tag{20b}$$

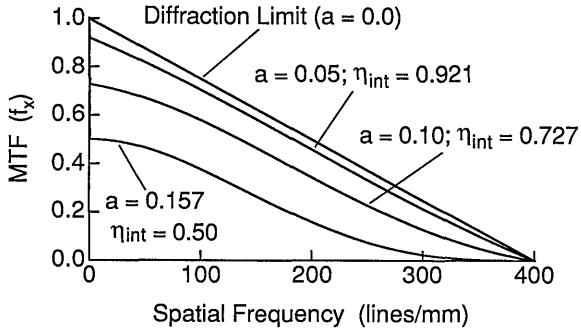

Fig. 4. Modulation transfer functions (MTF's) for the imaging example. The wavelength is 0.5 μm and the system f-number is $F/5$.

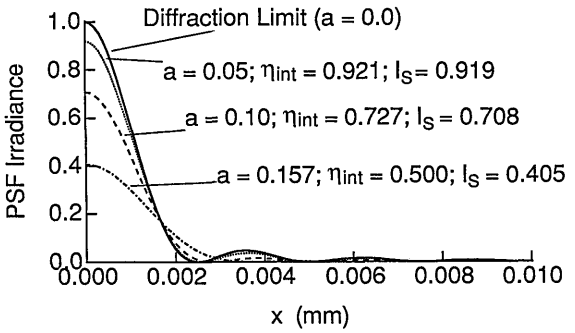

Fig. 5. Point-spread functions (PSF's) for the imaging example. I_S is the value of the Strehl intensity for each value of a.

Equations (20) are normalized such that $I(0) = 1.0$ for $a = 0$. Taking the Fourier transform of Eqs. (20) gives the OTF

$$\mathrm{OTF}(f_x) = \frac{1}{2D}\left\{(D - \lambda R f_x)\cos(a\lambda R f_x) + \frac{\sin[a(D - \lambda R f_x)]}{a} + \frac{\sin(\pi D f_x)}{\pi f_x}\right\}$$

$$- \frac{1}{2D}\left\{\frac{\sin[D(a - \pi f_x)]}{2(a - \pi f_x)} + \frac{\sin[D(a + \pi f_x)]}{2(a + \pi f_x)}\right\},$$

$$|f_x| \le D/(\lambda R). \tag{21}$$

The first two terms in the expression for the OTF are caused by the $m = 1$ diffraction order; we can see that these two terms are equal to η_{int} given by Eq. (19) for $f_x = 0$.

For example values of $R = 100$ mm, $D = 20$ mm, and $\lambda = 0.5$ μm, the OTF(f_x) as given by Eq. (21) is shown in Fig. 4 for several values of a. This figure demonstrates the results of the previous section: η_{int} is the limiting value for the OTF for low spatial frequencies and η_{int} acts as a scale factor for the entire transfer function. For the larger values of a, one can see the apodization-like effects of the local diffraction efficiency. One must look at spatial frequencies of less than one-half line/mm to see a significant nonzero contribution from the BG term to the OTF.

The point-spread functions for this example case are shown in Fig. 5. Also, Table 1 provides additional data derived from these spread functions: FWHM is the full width of the spread function at the half-power points and EE is the fractional energy

Table 1. Integrated Efficiency, Full-Width-at-Half-Power Points, and Energy Enclosed Within the First Zeros of the Diffraction-Limited Point-Spread Function for the Example Pupil Functions Described in the Text

a	η_{int}	FWHM(μm)	EE(x = 2.5 μm)
0.0	1.0	2.215	0.903
0.05	0.921	2.256	0.846
0.10	0.727	2.410	0.698
0.157	0.500	2.972	0.485

enclosed within ± 2.5 μm of $x = 0$ (The first zero of the diffraction-limited point-spread function is at $x = \pm 2.5$ μm). This data shows that some care must be taken in choosing a meaningful merit function for diffractive optics. For example, in this case the FWHM increases only slightly, but EE decreases by almost a factor of 2 for a change in η_{int} from 1.0 to 0.5. Hence FWHM is not a good metric to characterize the performance of a diffractive lens.

5. Polychromatic Integrated Efficiency

In general, the efficiency of a diffractive structure will be a function of the wavelength of the light.[5] If there are diffractive optics in a system that utilizes spectrally broadband illumination, the wavelength dependence of the diffraction efficiency must be considered when evaluating imaging performance. To determine the polychromatic transfer function for a diffractive lens, we first need to define a polychromatic integrated efficiency for the wavelength band ranging from λ_{min} to λ_{max}. This quantity is defined in a manner similar to η_{int}, except now the integration is over wavelength rather than over the pupil plane coordinates. Denoting the integrated efficiency at wavelength λ by $\eta_{int}(\lambda)$, we find that the polychromatic integrated efficiency is

$$\eta_{int,poly} = \frac{\int_{\lambda_{min}}^{\lambda_{max}} \eta_{int}(\lambda)d\lambda}{\lambda_{max} - \lambda_{min}}. \quad (22)$$

In general, $\eta_{int}(\lambda)$ will be a pupil-averaged integrated-efficiency value for each wavelength. The polychromatic optical transfer function, OTF_{poly}, is defined as the spectral average of the monochromatic transfer functions[17]

$$OTF_{poly}(f_x, f_y) = \frac{\int_{\lambda_{min}}^{\lambda_{max}} S(\lambda)OTF(f_x, f_y; \lambda)d\lambda}{\int_{\lambda_{min}}^{\lambda_{max}} S(\lambda)d\lambda}, \quad (23)$$

where $S(\lambda)$ denotes the spectral distribution and responsivity of the source–detector combination. For a diffractive lens, the polychromatic OTF is the value of the transfer function, relation (16), spectrally averaged over the desired wavelength band. Denoting the polychromatic transfer function, including the effects, if any, of the $S(\lambda)$ term, corresponding to the $m = 1$ order by $OTF_{m=1,poly(f_x,f_y)}$, and using similar reasoning as for the monochromatic case, we find an approximate polychromatic transfer function given by

$$OTF_{poly(f_x,f_y)} \cong \eta_{int,poly}OTF_{m=1,poly(f_x,f_y)} + (1 - \eta_{int,poly})\delta_{f_x,0}\delta_{f_y,0}. \quad (24)$$

Note that one additional approximation is used in the derivation of relation (24)—the average of the product $\eta_{int}(\lambda)OTF(\lambda)$ is approximately equal to the product of the averages of the two individual terms.

In many cases, the diffractive component or components of broadband systems will be weakly powered because of the large chromatic dispersion of diffractive optics. In these situations, the wavelength-to-grating period ratios will be small across the entire lens and the scalar predictions of diffraction efficiency are valid. If this is the case, we can provide an explicit expression for $\eta_{int,poly}$. The scalar-diffraction-theory value for the diffraction efficiency in order m for wavelength λ is given by (ignoring the small effect of the dispersion of the lens material)[18]

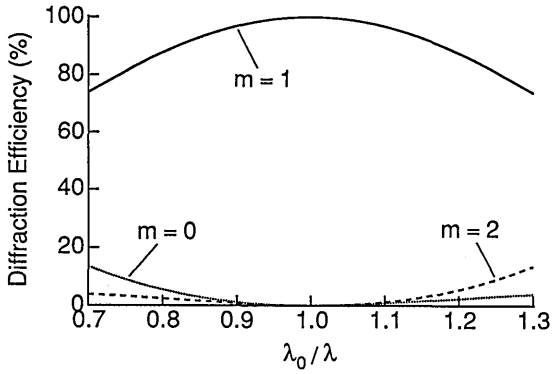

Fig. 6. Scalar value of the diffraction efficiency η_{scalar} as a function of the wavelength-detuning parameter λ_0/λ for the diffraction orders $m = 0$, 1, and 2.

$$\eta_{scalar}(\lambda) = \frac{\sin^2\left[\pi\left(\frac{\lambda_0}{\lambda} - m\right)\right]}{\left[\pi\left(\frac{\lambda_0}{\lambda} - m\right)\right]^2}, \quad (25)$$

where λ_0 is the design wavelength for the lens. Figure 6 is an illustration of Eq. (25) for $m = 0$, 1, and 2. The expression for $\eta_{scalar}(\lambda)$ given by Eq. (25) cannot be explicitly integrated, but an approximate expression for $\eta_{int,poly}$ can be found by expanding $\eta_{scalar}(\lambda)$ in a power series and integrating term by term. The resulting approximate expression, assuming $m = 1$, is

$$\eta_{int,poly} \cong 1 + \frac{\pi^2}{3\lambda_0}(\lambda_{min} + \lambda_{max} - \lambda_0) - \frac{\pi^2}{9\lambda_0^2}(\lambda_{min}^2 + \lambda_{min}\lambda_{max} + \lambda_{max}^2). \quad (26)$$

Table 2 provides some examples of the validity of the approximation of relation (26). The table compares the value of $\eta_{int,poly}$ given by relation (26) and by numerical integration of Eq. (25) for $m = 1$.

Table 2. Approximate[a] and Exact[b] Polychromatic Integrated Efficiencies for Several Spectral Regions, Based on the Scalar Prediction of Diffraction Efficiency

λ_0 (μm)	λ_{min} (μm)	λ_{max} (μm)	$\eta_{int,poly}$[a]	$\eta_{int,poly}$[b]
0.55	0.40	0.70	0.9184	0.9139
4.0	3.0	5.0	0.9315	0.9281
10.0	8.0	12.0	0.9561	0.9546

[a]From relation (26).
[b]Numerical integration of Eq. (25).

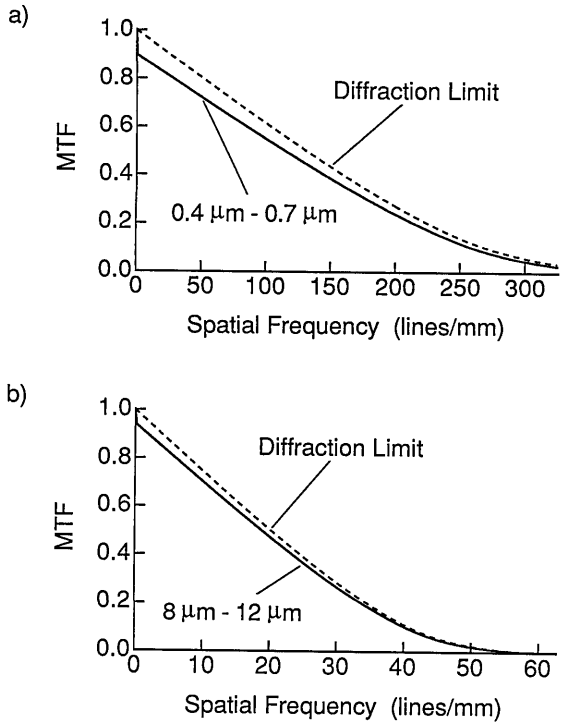

Fig. 7. Polychromatic modulation transfer functions (MTF's) for two spectral bands. a)$F/5$ system (circular exit pupil) with a center wavelength of $\lambda_0 = 0.55$ μm and a spectral bandwidth of 0.40–0.70 μm. The value of $\eta_{int,poly}$ is 0.914. b) $F/2$ system (circular exit pupil) with a center wavelength of $\lambda_0 = 10.0$ μm and a spectral bandwidth of 8.0–12.0 μm. The value of $\eta_{int,poly}$ is 0.955.

Figure 7 shows polychromatic transfer functions calculated by using the scalar expression for diffraction efficiency, Eq. (25). The resulting curves show the behavior predicted by the approximate expression of relation (24): the $m = 1$ polychromatic OTF scaled by $\eta_{int,poly}$ and a zero-frequency spike.

6. Conclusion

We have presented an analysis of the OTF achievable with diffractive lenses that have a nonunity diffraction efficiency. These losses in diffraction efficiency may be a result of high wavelength-to-grating period ratios (departures from scalar-diffraction conditions), manufacturing inaccuracies, or, in the case of broadband systems, wavelength detunings from the design wavelength. It is seen that the integrated efficiency, η_{int}, can be served as a useful one-number merit function for describing the diffraction efficiency of diffractive optical elements. A complete characterization of an optical system that contains one or more diffractive components should include, in addition to conventional aberration analysis, an evaluation of η_{int}, which will generally be a function of field position. Because the presence of the background orders is a real component of a diffractive system, interferometric and spread-function testing optics may give differing results, depending on how the background orders are handled in the analysis.[19] Because η_{int} is the fractional energy in the order of interest that reaches the image plane, the deleterious effects of the background orders may be reduced by careful system design, permitting as much as possible of the background orders to be vignetted out of the system. This reduction, of course, does not increase the diffraction efficiency of the lens itself, but it may increase the value of η_{int} measured in the pupil. The concept of integrated efficiency is easily extended to the polychromatic case by defining a wavelength-integrated polychromatic integrated efficiency, $\eta_{int,poly}$, which acts as a scale factor for the polychromatic transfer function.

APPENDIX A. Evaluation of Cross Terms in Eq. (5)

Let us consider the cross terms in Eq. (5) more carefully. In many cases the diffractive lens pupil function will be represented by a Fourier series. For simplicity, consider a one-dimensional function $f(x)$ of period L. We can write $f(x)$ as the Fourier series

$$f(x) = \sum_{m=-\infty}^{\infty} c_m \exp(i2\pi m f_0 x), \tag{A1}$$

where $f_0 = 1/L$. If $f(x)$ is a pure phase function, as is the case for a nonabsorbing diffractive lens, then $|f(x)| = 1$. Let us further assume that $f(x) \equiv 0$ for $|x| > (D/2)$ and that the interval $-D/2 \le x \le D/2$ contains an integral number of periods L, so that the Fourier series expansion is valid everywhere in $-D/2 \le x \le D/2$. In other words, $D = NL$, where N is a positive integer. By Parseval's identity for Fourier series,

$$\frac{1}{L}\int_0^L |f(x)|^2 dx = \sum_{m=-\infty}^{\infty} |c_m|^2. \tag{A2a}$$

For our case of $|f(x)|^2 = 1$, Eq. (A2a) reduces to

$$\sum_{m=-\infty}^{\infty} |c_m|^2 = 1 \qquad \text{for } |x| \le D/2. \tag{A2b}$$

Equations (A2) are a statement of conservation of energy. Let us denote the Fourier transform of $f(x)$ by $F(f_x)$. Taking the transform of Eq. (A1) and recalling that $f(x)$ is zero outside $|x| \le (D/2)$, we can write

$$F(f_x) = \sum_{m=-\infty}^{\infty} c_m D \,\mathrm{sinc}[D(f_x - mf_0)], \tag{A3}$$

where $\mathrm{sinc}(x) \equiv \sin(\pi x)/(\pi x)$. The squared modulus of $F(f_x)$ is

$$|F(f_x)|^2 = \sum_{m=-\infty}^{\infty} |c_m|^2 D^2 \,\mathrm{sinc}^2[D(f_x - mf_0)] + \sum_{\substack{m,n=-\infty \\ m\neq n}}^{\infty} (c_m c_n^*) D^2 \times \mathrm{sinc}[D(f_x - mf_0)]\mathrm{sinc}[D(f_x - nf_0)]. \tag{A4}$$

The total energy in $F(f_x)$ is found by the integration of Eq. (A4). Integration of the sinc functions in the second term on the right-hand side of Eq. (A4) yields

$$\int_{-\infty}^{\infty} D^2 \operatorname{sinc}[D(f_x - mf_0)] \operatorname{sinc}[D(f_x - nf_0)]df_x = D \operatorname{sinc}[Df_0(m - n)]. \quad \text{(A5)}$$

Note, however, that $Df_0 = D/L = N$, so the argument of the sinc function in Eq. (A5) is $N(m - n)$, which is always a nonzero integer for $m \neq n$. Because the sinc function is zero for nonzero integer values of its argument, we see that the cross terms in the integration of Eq. (A4) integrate to zero, i.e., they have no contribution to the total energy in $F(f_x)$.

If the pupil function for the diffractive lens is given as an expansion in an orthogonal basis set, such as a Fourier series, the above analysis reveals that the cross terms in Eq. (5) contain no energy:

$$\int_{-\infty}^{\infty}\int_{-\infty}^{\infty} h_{m=1}^*(x, y)h_{BG}(x, y)dxdy = \int_{-\infty}^{\infty}\int_{-\infty}^{\infty} h_{m=1}(x, y)h_{BG}^*(x, y)dxdy = 0. \quad \text{(A6)}$$

At each point (x, y) in the image plane, $h_{m=1}^*(x, y)$ $h_{BG}(x, y)$ and $h_{m=1}(x, y)$ $h_{BG}^*(x, y)$ may be nonzero and contribute to the irradiance at that point, but because they always integrate to zero, they do not affect the value at the origin of the OTF. [See Eq. (12).] Also, as we discussed in Section 3, because $h_{m=1}(x, y)$ and $h_{BG}(x, y)$ will usually have a much different spatial extent and the cross terms in Eq. (5) are essentially a measure of the overlap of $h_{m=1}(x, y)$ and $h_{BG}(x, y)$, the magnitude of $h_{m=1}^*(x, y)$ $h_{BG}(x, y)$ and $h_{m=1}(x, y)$ $h_{BG}^*(x, y)$ will usually be small. For these reasons, we ignore these cross terms in the analysis following Eq. (5).

This research was supported in part by the New York State Center for Advanced Optical Technology. D. A. Buralli gratefully acknowledges the support of the Kodak Fellows Program. Portions of this research were presented as paper TuJ2 at the 1990 annual meeting of the Optical Society of America, Boston, Mass., 4–9 November 1990.

References and Notes

1. P. P. Clark and C. Londoño, "Production of kinoforms by single point diamond machining," Opt. News, **15,** 39–40 (1989); J. A. Futhey, "Diffractive bifocal intraocular lens," in *Holographic Optics: Optically and Computer Generated,* I. Cindrich and S. H. Lee, eds., Proc. Soc. Photo-Opt. Instrum. Eng. **1052,** 142–149 (1989); G. M. Morris and D. A. Buralli, "Wide field diffractive lenses for imaging, scanning, and Fourier transformation," Opt. News **15**(12), 41–42 (1989).
2. L. d'Auria, J. P. Huignard, A. M. Roy, and E. Spitz, "Photolithographic fabrication of thin film lenses," Opt. Commun. **5,** 232–235 (1972); G. J. Swanson and W. B. Veldkamp, "Diffractive optical elements for use in infrared systems," Opt. Eng. **28,** 605–608 (1989).
3. V. P. Koronkevich, "Computer synthesis of diffraction optical elements," *Optical Processing and Computing,* H. H. Arsenault, T. Szoplik, and B. Macukow, eds. (Academic, Orlando, Fla., 1989), pp. 277–313.
4. For example, see the proceedings of several recent conferences on holographic and diffractive optics: Proc. Soc. Photo-Opt. Instrum. Eng. **883, 1052, 1136, 1211,** and selected papers in Proc. Soc. Photo-Opt. Instrum. Eng. **1354.**
5. D. A. Buralli, G. M. Morris, and J. R. Rogers, "Optical performance of holographic kinoforms," Appl. Opt. **28,** 976–983 (1989).
6. There are many papers that describe results from the rigorous electromagnetic grating theory. See, for example, E. G. Loewen, M. Nevière, and D. Maystre, "Grating efficiency theory as it applies to blazed and holographic gratings," Appl. Opt. **16,** 2711–2721 (1977); R. Petit, ed., *Electromagnetic Theory of Gratings,* (Springer-Verlag, Berlin, 1980).
7. K. Rosenhauer and K. Rosenbruch, "Flare and optical transfer function," Appl. Opt. **7,** 283–287 (1968).
8. O. A. Barteneva, "Effect of scattered light on the photographic image quality," Sov. J. Opt. Technol. **44,** 197–199 (1977).
9. J. J. Jakubowski, "Methodology for quantifying flare in a microdensitometer," Opt. Eng. **19,** 122–131 (1980).
10. J. W. Goodman, *Introduction to Fourier Optics* (McGraw-Hill, San Francisco, Calif., 1968), pp. 90–96.
11. W. B. Wetherell, "The calculation of image quality," in *Applied Optics and Optical Engineering,* R. R. Shannon and J. C. Wyant, eds. (Academic, Orlando, Fla., 1980), Vol. VIII, pp. 202–215.
12. G. J. Swanson, "Binary optics technology: the theory and design of multi-level diffractive optical elements," Tech. Rep. 854 (Lincoln Laboratory, MIT, Lexington, Mass., 1989); W. -H. Lee, "Computer-generated holograms: techniques and applications," in *Progress in Optics XVI,* E. Wolf., ed. (North-Holland, Amsterdam, 1978).
13. Similar transfer functions for zone plates have been published in M. J. Simpson and A. G. Michette, "Considerations of zone plate optics for soft x-ray microscopy," Opt. Acta **31,** 1417–1426 (1984) and in A. G. Michette, *Optical Systems for Soft X-Rays* (Plenum, New York, 1986), pp. 186–188.
14. J. A. Cox, T. Werner, J. Lee, S. Nelson, B. Fritz, and J. Bergstrom, "Diffraction efficiency of binary optical elements," in *Computer and Optically Formed Holographic Optics,* I. Cindrich and S. H. Lee, eds., Proc. Soc. Photo-Opt. Instrum. Eng. **1211,** 116–124 (1990).
15. D. A. Buralli and G. M. Morris, "Design of two- and three-element diffractive Keplerian telescopes," Appl. Opt. **31,** 38–43 (1992).
16. Ref. 10, pp. 70–74.
17. Ref. 11, pp. 225–226.
18. See Eq. (11) of Ref. 5.
19. J. P. Jennings, F. J. Busselle, and S. G. Shaw, "Observed differences in MTF results between line-spread and interferometric measurements for IR lenses," in *Infrared Technology and Applications,* L. R. Baker and A. Masson, eds., Proc. Soc. Photo-Opt. Instrum. Eng. **590,** 138–143 (1985).